scientific reports

Check for updates

OPEN

Tolerability and effect of inhibiting microfibrillar-associated protein 4 in small intestinal anastomotic healing

Rasmus Refshauge Andresen[1,6,7], Jesper Brandt Pedersen[1,6,7], Paula Frederikke Hellsegg Grünfeld[1,6], Charlotte Skoie Nielsen[1,6], Anna Lings Kjelgaard[1,6], Anders Frederik Højer Kolind[1,6], Nils Grimm[1,6], Kasper Emil Rosenbech[1,6], Henriette Kirkeby Høiberg[1,6], Johanne Kalland[1,6], Mie Dilling[1,6], Gunvor Iben Madsen[2], Anders Schlosser[3], Lasse Bach Steffensen[3], Hans Christian Beck[4], Sören Möller[5], Niels Qvist[1,6], Mark Ellebæk[1,6,8]✉ & Grith Lykke Sorensen[3,8]

Crohn's disease often leads to strictures due to excessive extracellular matrix deposition and smooth muscle cell hyperplasia. Current stricture treatments include surgical and endoscopic interventions, but high recurrence rates remain a challenge. Microfibrillar-associated protein 4 (MFAP4) contributes to fibrosis in various tissues. The anti-MFAP4 antibody was evaluated for its tolerability and anti-fibrotic efficacy on small intestinal anastomotic healing in pig models. Two small intestinal anastomoses were made in 45 pigs. Fibrosis was induced using aethoxysklerol injections. Each anastomosis was locally injected with either anti-MFAP4, positive control anakinra (interleukin-1 receptor antagonist) or negative vehicle control. Tolerability of anti-MFAP4 was observed across three observation durations (5, 10, and 28 days) and assessed by weight gain, anastomotic tissue strength, and histological evaluation. Anti-fibrotic efficacy was tested using semi-quantitative collagen scoring from the 28-days study. Proteome analysis of tissue sections was applied for mechanistic analyses. Local anastomotic injections of 16 mg and 32 mg anti-MFAP4 were well tolerated. Anastomotic fibrosis was significantly reduced both by positive control anakinra-treatment and anti-MFAP4-treatment. Anti-MFAP4 reduced fibrosis by 23% relative to the negative control. Gene ontology term analysis showed up-regulation of muscle cell contractile apparatus and down-regulation of transcription and translation in the anti-MFAP4 group. The data supported that anti-MFAP4-treatment reduced the anastomotic collagen deposition compared with vehicle. Moreover, the treatment induced smooth muscle cell switching from the synthetic phenotype involved in fibrosis to the contractile phenotype essential for homeostatic gut motor activity.

Keywords Intestinal anastomoses, Microfibrillar-associated protein 4, Fibrosis, Smooth muscle cells, Phenotype switch

Abbreviations

CD	Crohn's disease
ECM	Extracellular matrix
SMC	Smooth muscles cells
MFAP4	Microfibrillar-associated protein 4
scRNA-seq	Single-cell RNA sequencing

[1]Research Unit for Surgery, Odense University Hospital, Odense, Denmark. [2]Department of Pathology, Odense University Hospital, Odense, Denmark. [3]Institute of Molecular Medicine, University of Southern Denmark, Odense, Denmark. [4]Centre for Clinical Proteomics, Department of Clinical Biochemistry, Odense University Hospital, 5000 Odense, Denmark. [5]Research Unit OPEN, Odense University Hospital, Odense, Denmark. [6]University of Southern Denmark, Odense, Denmark. [7]These authors are contributed equally: Rasmus Refshauge Andresen and Jesper Brandt Pedersen. [8]These authors are jointly supervised this work: Mark Ellebæk and Grith Lykke Sorensen. ✉email: Mark.Ellebaek1@rsyd.dk

IL-1Ra	Interleukin-1 receptor antagonist
AI	Anastomotic index
MATS	Maximal anastomotic tensile strength
FOXP3	Forkhead box P3
α-SMA	α-Smooth muscle actin
TBS	Tris-buffered saline
PBS	Phosphate-buffered saline
BSA	Bovine serum albumin
RIPA	Radioimmunoprecipitation assay
HRP	Horseradish peroxidase
OPD	O-phenylenediamine dihydrochloride
CRTAP	Cartilage Associated Protein
COL2A1	Collagen type II alpha 1 chain
COL3A1	Collagen type III alpha 1 chain
OLMF4	Olfactomedin 4
PKM	Pyruvate Kinase M
GO	Gene Ontology
GAIN	Gastrointestinal diseases and malformations in infancy and childhood

Crohn's disease (CD) is a type of inflammatory bowel disease characterized by chronic transmural inflammation, most commonly affecting the terminal ileum[1]. The inflammation may lead to intestinal wall fibrostenosis, and up to 70% of the Crohn's disease patients will develop fibrotic stricture at 10 years after diagnosis[2]. Fibrostenotic complications are the most common driver for intestinal resection. After introduction of biologics then cumulative 5-year resection rate decreased from 12,5% to 9,3% after diagnosis[3]. A similar trend in the re-resection rate has been demonstrated. The disease-driven re-resection rates after 1, 5 and 10-years was 3,6%, 10,1% and 14,1% respectively in a population study[4].

The development of intestinal strictures in CD is multifactorial. Aberrant inflammatory wound healing characterized by excessive collagen-rich extracellular matrix (ECM) deposition by increased numbers of mesenchymal cells is one factor and smooth muscles cell (SMC) hyperplasia/hypertrophy is another important factor[5,6]. SMC are recognized with the capacity to dedifferentiate from a normal contractile, quiescent phenotype to a synthetic phenotype characterized with increased ECM synthesis and proliferation during wound healing and pathophysiological conditions[7]. Excessive SMC proliferation has been demonstrated in both Crohn's strictures[8] as well as in animal models of induced intestinal inflammation[9] and is recognized as the most prominent histological change in crohn's fibrostenosing strictures[5]. The pathophysiological process includes increasing expression of integrin $\alpha_V\beta_3$, which has been shown to increase SMC proliferation and hyperplasia in stricturing CD[8].

In the earliest phase of wound healing (day 1–4) hemostasis results in clot-formation and the release of pro-inflammatory cytokines. Inflammation is induced by the cytokines and the accumulation of apoptotic and necrotic cellular material followed by migration of neutrophiles and macrophages. This is followed by a proliferative phase (day 4–14) where mesenchymal cells migrate into the healing tissue and start to proliferate. These cells; including fibroblasts, myofibroblasts and SMCs, are responsible for the formation of collagen. The resulting collagen deposition provides anastomotic strength and stability and the tissue continuity is dynamically restored during this phase[10]. Also, a shift from pro- to anti-inflammatory signaling restricts the inflammatory response in this phase. In the final remodeling phase (day 14 →), deposited collagen is remodeled by fibrolytic activity. Collagen type III is partly replaced with the more durable collagen type I and tissue strength is plateaued[11]. A disturbed wound healing from an underlying disease such as CD may result in the formation of excessive extracellular matrix resulting in a fibrotic stenosis in the anastomotic area and recurring after surgical resection[6].

The ECM protein microfibrillar-associated protein 4 (MFAP4) co-localizes with elastin and collagen fibers, especially in small intestine, the heart, and lungs[12–14]. MFAP4-deficiency is demonstrated to be protective of development of fibrosis in heart and kidney[15–17]. Recently, an animal model of inflammatory bowel disease showed that MFAP4 colocalizes with fibrotic markers suggesting it to also be a profibrotic driver in the intestines[18]. MFAP4 is found significantly increased in response to TGF-β treatment in human mesenchymal cells[19], and in line with this, transcriptomic analysis has demonstrated that MFAP4 is expressed in SMC, fibroblasts and activated fibroblasts in ileal resections from CD patients[18].

The above observations provides the rationale for testing the role of MFAP4 in intestinal fibrostenotic processes.We hypothesized that MFAP4 could serve as therapeutic target in anastomotic fibrostenotic processes.

We have previously developed an anti-MFAP4 antibody with the capacity to block MFAP4 binding to integrin $\alpha_V\beta_3$ and the consective activation of integrin expressing cells[20]. We tested if local pharmacological treatment with anti-MFAP4 was tolerated, tested therapeutic efficacy of reducing fibrosis in pig intestinal anastomotic healing, and investigated the therapeutic effects by proteome analysis.

Materials and methods

Ethical approval

All experiments were performed in accordance with relevant guidelines and regulations, and all live animal experimental protocols were conducted according to ARRIVE 2.0 guidelines[21] and were approved by the Danish Animal Experiments Inspectorate (j. nr. 2018–15-0201–01,583).

Study design

Three separate interventional randomized and investigator blinded studies were performed using Danish Landrace pigs. In each study two hand sewn anastomoses were created in the small intestines. The different lengths of the studies, 5 days, 10 days and 28 days, were chosen for the observation of tolerability of injecting anti-MFAP4 in the different phases of wound healing[10]. Tolerability outcomes were anastomotic healing following initial inflammatory healing phase with provisional wound closure (Day 5), during the proliferative phase where the tissue strength is dynamically restored (Day 10) and during the remodeling phase (Day 28). The tolerability was evaluated through patological scoring, macroscopical findings, measurements of tissue strength and formation of adherences. The primary efficacy outcome was collagen-deposition following anti-MFAP4 treatment observed in the 28-days study. The secondary outcome was therapeutic mechanisms evoked by anti-MFAP4 in the 28-days study and observed by proteome analysis .

5-days study: Each pig received either vehicle control treatment (n = 6) or anti-MFAP4 treatment (20 mg/ml) (n = 7). A total of 0.8 ml of vehicle or anti-MFAP4 was injected in 8 predefined subserosal depots on each side of the anastomosis at a distance of 2 mm from the anastomotic line. Pigs were euthanized at postoperative day 5 and the anastomotic site was resected. After a tensile strength test the anastomotic tissues was fixed in formalin for later histological examination.

10-days study: All pigs received aethoxysklerol (5 mg/ml) injections with a total of 0.8 ml distributed on 8 predefined subserosal depots on both sides of the anastomotic side together with either vehicle control treatment (n = 7) or anti-MFAP4 treatment (20 mg/ml) (n = 7) as described in the 5-days study. Pigs were euthanized on postoperative day 10. The anastomotic area was resected after in situ contrast study (X-ray). After a tensile strength test the anastomotic tissue was fixed in formalin for later histological examination.

28-days study: In all pigs, aethoxysklerol injections was performed as described above. On postoperative day 14, a re-laparotomy was performed, and the pigs were randomized to receive either positive control anakinra (Interleukin-1 receptor antagonist (IL-1Ra)) treatment (40 mg/ml) (n = 9), vehicle control treatment (n = 9), or anti-MFAP4 treatment (40 mg/ml). In total, a volume of 0.8 ml of each was injected around the anastomotic area as described above. On postoperative day 28, in situ contrast study (X-ray) of the anastomotic area was performed, and the anastomotic area was resected. After a tensile strength test the anastomotic tissue was fixed in formalin for later histological examination.

Figure 1 summarizes the study outline.

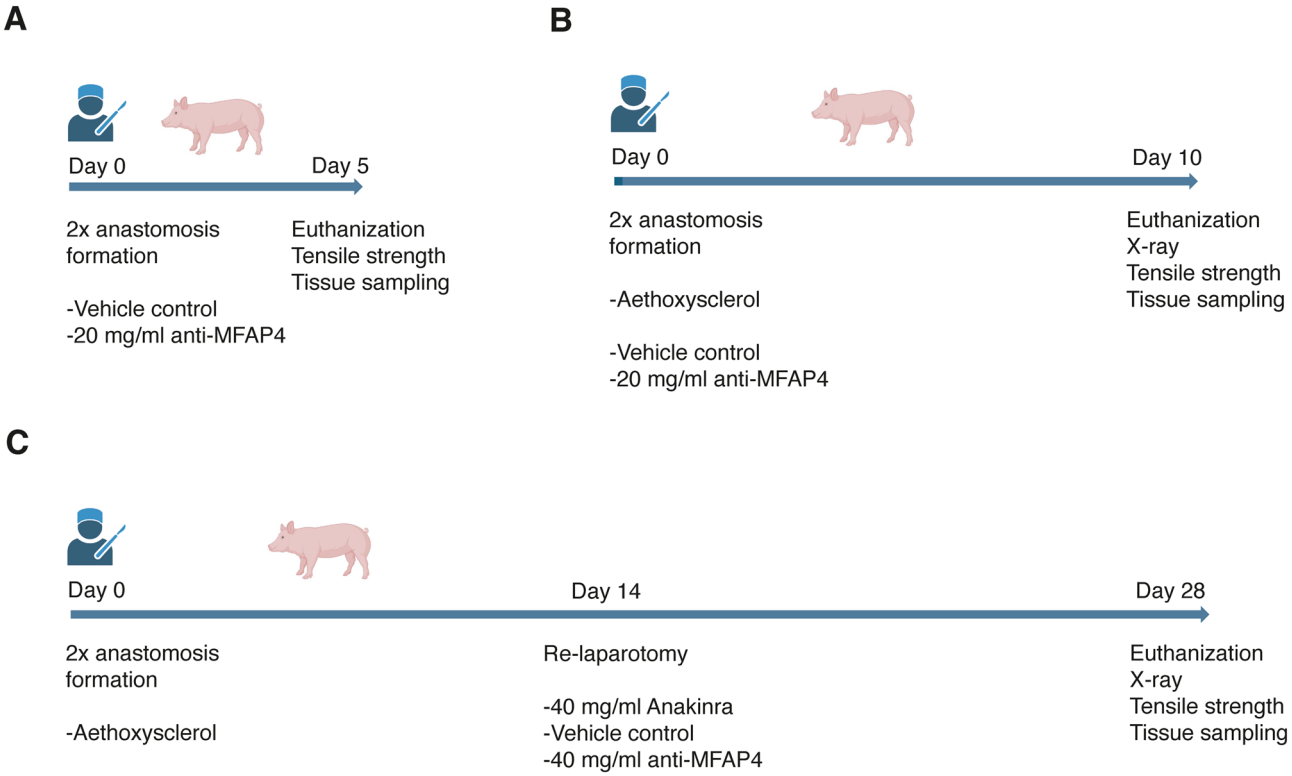

Fig. 1. Study outline. Three interventional studies of pig anastomosis healing were performed. In each study two hand sewn anastomoses were created in the small intestines on day 0. The length of the studies was varied to allow observation of tolerability of intervention (**A**, 5-days study) following the initial inflammatory healing phase with provisional wound closure, (**B**, 10-days study) during the proliferative phase where the tissue strength is dynamically restored, and (**C**, 28-days study) following the proliferative phase of healing. The sclerotic agent aethoxyklerol and anakinra was used to induce fibrosis and as positive anti-fibrotic treatment control, respectively. Image is created using BioRender.

Animals

Weaned female Danish Landrace & Yorkshire pigs (obtained from the breader Kokkenborg, Stenstrup, Denmark) of approximately 20 kg were included in the study. The pigs were acclimatized to their new environment for at least one week prior to surgery. They were housed at a conventional large animal housing facility with light/dark cycles (twelve hours with gradually dimmed light and natural light from windows) at a constant temperature of 20–21 °C. The pigs had access to food twice daily (0.9 kg/20 kg body weight) and free access to water. Before surgical procedures the pigs were weighed. To ensure animal welfare, the pigs were intensively inspected daily, and during the first 24 h following surgery.

Anesthesia

Prior to anesthesia the pigs were sedated, and the general anesthesia was induced by an infusion of propofol. The pigs were mechanically ventilated. Blood pressure, electrocardiogram, heart rate and oxygen saturation were monitored and profylactic antibiotics were administered pre- and postoperatively. The postoperative analgesia consisted of a fentanyl transdermal patch and either intramusculary injection of buprenorphine every four to six hours in the first 24 h after surgery for the 5- and 10-days study, or a subcutaneous injection of sustained-release formulation of buprenorphine preoperatively for the 28-days study. All pigs were euthanized using 140 mg/kg pentobarbital (400 mg/ml).

Full description of anesthesia and euthanization is in the supplementary method section.

Surgery

During surgery, the pigs were placed on a heating pad set to 32 °C, to avoid hypothermia. They received Ringer's acetate i.v. at a rate of 4–10 ml/kg/h. The small intestines were exposed through a 10 cm lower midline laparotomy. Two end-to-end anastomoses were created 50 cm and 150 cm orally to the ileoceacal junction with a seromuscular running suture using monocryl 4–0 (Ethicon, Johnson & Johnson, Diegem, Belgium). After interventional procedures the abdominal fascia was closed with running PDS*II® 0 (Ethicon, Johnson & Johnson, Somerville, New Jersey, USA). The skin was closed intracutaneously with a running monocryl® 3–0 (Ethicon, Johnson & Johnson, Diegem, Belgium). The skin incision was sealed with a liquid bandage (KRUUSE Wound Plast, Cat. no: 161020).

At study completion, a re-laparotomy was performed, and all the anastomoses were identified and freed from adhesions, which were graded in using a modified Leach grading of adhesion (Supplemental Table S2). All anastomoses were examined for macroscopical findings such as pseudo-diverticulosis, abscesses, visible leakage, fistulas, or signs of ileus.

In 5 pigs, anastomotic tissue, lung, and artery biopsies from the 28-days study were collected at end-study for analysis of anti-MFAP4 deposition. An incision in the right diaphragmatic dome allowed harvesting of the biopsy from the basis of the middle lobe of the right lung. The arterial biopsy was harvested from the left common iliac artery. Biopsies were snap frozen with liquid nitrogen, and stored at -80 °C.

Interventional agents and controls

Anti-MFAP4 is a humanized, monoclonal IgG1 antibody, that binds to MFAP4 with high affinity and blocks its interaction with integrins[20]. Wild-type anti-MFAP4 was used for the 5-days and the 10-days study. For the 28-days study, we applied a point-mutated variant with minimized Fc-mediated effects the so-called hIgG1-P329G LALA variant[20]. Aethoxysclerol® (Kreussler Pharma) causes submucosal fibrosis by local injection[22]. The positive control was anakinra (40 mg/mL, Kineret®. Swedish Orphan Biovitrum. Batch 3798201c), vehicle control (10 mM histidine, 10% w/w trehalose pH 6.0), or anti-MFAP4 (20 or 40 mg/mL). For both anti-MFAP4- and aethoxysklerol-treatment and for control-treatments (vehicle and anakinra) a volume of 0.8 ml was injected into the anastomotic area.

Radiography

The wound contraction at the anastomotic site was assessed in situ by a contrast study. The intestinal loop was clamped approximately 10 cm proximally and distally to each anastomosis. Water-soluble contrast (Omnipaque®, GE HealthCare) was infused to a pressure of 20 mmHg and an image in one plane was obtained. The intestinal diameters were measured orally and aborally to the anastomotic site using an image analysis software (Image J, NIH, Bethesda, USA). An anastomotic index (AI) was calculated for each anastomosis by dividing the diameter of the anastomosis sites by a mean pre- and postanastomotic diameter based on five measure points at 1 cm intervals from the anastomotic line (Supplemental Figure S2).

Maximal anastomotic tensile strength (MATS)

Following radiography, the anastomosis was resected with approximately 5 cm margin orally and aborally and cleaned of fecal contents with water prior to maximal anastomotic tensile strength (MATS) test. The resected intestinal segment was mounted by two clamps in the tensile testing machine (LF Plus®; Lloyds Instruments, Fareham, UK) equipped with an XCL 100 N loadcell (Lloyds Instruments, Fareham, UK) 5 min after resection to prevent the influence of cold ischemia. The position of the clamps was in a distance of 6 cm with the anastomosis placed in the center (Supplemental Figure S3). The segment was gradually stretched at a constant deformation rate of 15 mm/min until rupture occurred.

The applied force in Newton was measured at three points:

1. When a tear became visible in the serosa (MATS 1).
2. When a transmural lesion was visible (MATS 2). The rupture was confirmed by a simultaneous drop in the load-strain curve calculated by the software NEXYGEN Plus ® (version 3.0; Lillerød, Denmark).

3. The maximal force applied during the tensile strength test (MATS 3) was calculated by the software.

Histological procedure and assessment

A ten mm long intestinal tissue section with central intact anastomotic line was prepared and fixed in a 4% formaldehyde solution for 48 h and subsequently embedded in paraffin. Three micrometer thick slices were stained with hematoxylin and eosin or picrosirius red for histological evaluation.

The anastomotic healing of each anastomosis was visually assessed according to the Verhofstad scale[23] (Supplemental Table S3), evaluating necrosis, polymorph nucleated cells, lymphocyte infiltration and macrophages, degree of edema, state of epithelial layer and bridging of the submucosal layer. Collagen deposition at the anastomotic line was scored in percentage of the anastomotic area. Each anastomosis was assessed independently using a mean score from two sections from the same anastomosis. Treatment group was blinded to the assessor.

Proteome analysis

Three µm sections of formalin-fixed, paraffin-embedded tissue from the distal anastomosis of each animal (n = 9/group) were deparaffinized by using xylene followed by extraction of proteins by dissolving the deparaffinized tissue sections in extraction buffer (1 M dithiothreitol (DTT), 0.2 M tetraethylammonium bicarbonate and 10% sodium dodecyl sulfate, then subjected to two rounds of ultra-sonification (15 min of ultra-sonification/15 min of cooling on ice), and incubated at 99 °C for 20 min then at 80 °C for 2 h. Protein alkylation was done by adding a 200 mM iodoacetamide (IAA) solution to a final DTT/IAA concentration ratio of 1:3. The acetone-precipitated proteins were re-dissolved in 5 µL 8 M urea with 1 µg LysC and incubated at 30 °C for 4 h, followed by a further dilution to 1 M urea, the addition of 2 µg trypsin, and an overnight incubation at 30 °C. The resulting tryptic peptide samples were isotopically labeled using the 16-plex tandem mass tag (TMTpro) (Thermo Fisher, USA) where a pool of all samples was labeled with the mass tag 126 that served as an internal standard. Tagged peptides were mixed into three mixed peptide samples that were fractionated into 7 fractions using high pH chromatography and analyzed by nano-HPLC-MSMS also as previously described[24] with the following modifications: LC gradient length was 100 min, higher-energy collisional dissociation was set to 36. All Thermo Scientific Exploris 480 raw data files were processed and quantified using Proteome Discoverer version 3.0 (Thermo Scientific, Waltham, MA, UnitedStates) using a combined Chimerys, Sequest and MS Amanda search. For Sequest and MS Amanda searches TMTpro (N-terminal and lysine) and cysteine carbamidomethylation set as fixed modifications, and methionine oxidation and asparagine and glutamine deamidation as variable modifications whereas for Chimerys TMTpro (N-terminal and lysine) and cysteine carbamidomethylation were set as fixed. Data were searched against the Uniprot pig proteome (Sus scrofa, UP000008227, 46,225 entries, downloaded 12th June 2024).

Pathway enrichment analyses were performed using clusterProfiler 4.0 package[25] and org.Hs.eg.db in R.

Immunohistochemistry

Three µm thick formalin-fixed, paraffin-embedded sections were mounted on FLEX IHC Microscope slides (Dako/Agilent, Glostrup, Denmark). Sections were dried at room temperature and baked at 60 °C for 60 min. Following, epitope retrieval was performed by processing samples in DISCOVERY Cell Conditioning solution (Ventana) for 32 min at 100 °C. Humanized anti-MFAP4 (human IgG) was detected by immunohistochemistry using Goat anti-Human IgG Fc (Abcam, Cambridge, UK, cat# ab ab97221) diluted 1:2000 and incubated for 32 min at 36 °C. Staining was automated using the Discovery Ultra immunostainer (Ventana Medical Systems, Tucson, AZ) and using the OmniMap anti-Goat-HRP detection system (Roche cat# 760–4647) followed by Discovery ChromoMap DAB (Ventana Medical Systems, Tucson, AZ). Nuclear counter staining was performed using Hematoxylin II (Ventana Medical Systems, Tucson, AZ). Finally, slides were washed, dehydrated, and coverslipped using an automated Dako coverslipper (Dako/Agilent, Glostrup, Denmark).

For α-smooth muscle actin (α-SMA) staining the tissues were processed as described above. Epitope retrieval was performed in Target Retrieval Solution-H (Agilent) for 30 min at 97 °C. Staining was performed using the OMNIS automated immunohistochemistry platform (Agilent) using mouse anti-α-SMA (BS66, Nordic Biosite, cat#BSH-7459) diluted 1:1,000 and detected using EnVision FLEX/HRP + Mouse LINK and EnVision FLEX DAB + Substrate Chromogen System (Agilent). Nuclear counter staining was performed using Hematoxylin, Mayers ready to use solution (Agilent). Finally, slides were washed, dehydrated, and cover slipped using an automated Dako cover slipper (Dako/Agilent, Glostrup, Denmark).

ELISA detection of anti-MFAP4 (human IgG) in tissue samples

Buffers: Tris-buffered saline (TBS): 140 mM NaCl (Merck Millipore), 10 mM Tris–HCl (Sigma-Aldrich), 0.02% (w/v) NaN_3 (Sigma-Aldrich), pH 7.4; TBS/Tw: TBS containing 0.05% (v/v) Tween 20 (polyoxyethylene sorbitan monolaurate, Merck Millipore); phosphate-buffered saline (PBS): 137 mM NaCl (Merck Millipore), 3 mM KCl (Merck Millipore), 8 mM Na_2HPO_4 (VWR) , 1.5 mM KH_2PO_4 (Merck Millipore), pH 7.4; PBS/Tw: TBS containing 0.05% (v/v) Tween 20 (polyoxyethylene sorbitan monolaurate, Merck Millipore); PBS/Tw/Bovine serum albumin (BSA): PBS/Tw, 0.1% BSA; substrate buffer: 35 mM citric acid (Sigma-Aldrich), 67 mM Na_2HPO_4 (VWR), pH 5.0.

Snap-frozen tissues from each of two anastomoses/pig, one pulmonary or arterial sample were included in ELISA analysis. 96-well MaxiSorp plates (NUNC MaxiSorp) were coated with in house produced recombinant MFAP4 (0.25 µg/ml in PBS) overnight at 4 °C, washed with PBS/Tw/BSA, and then blocked with PBS/Tw/BSA for 1 h at room temperature. To create a standard curve, Anti-MFAP4 was diluted to 10 ng/ml in PBS/Tw/BSA, followed by twofold dilutions in PBS/Tw/BSA. Intestinal, pulmonary and arterial tissues were homogenized in radioimmunoprecipitation assay (RIPA) buffer (Sigma-Aldrich cat#R0278) using a Precellys 24 tissue

homogenizer (Bertin Instruments) and protein concentrations of the lysates determined using the Biorad DC protein assay (Biorad cat nr 500,112). The lysates were diluted in PBS/Tw/BSA, to be within the linear range of the assay and aliquoted onto the MFAP4-coated plates (100 µl per well). All samples were incubated 1 h at room temperature, washed with PBS/Tw/BSA and incubated with horseradish peroxidase (HRP)-conjugated goat anti-human IgG (ab97225, Abcam) at 1:10,000 dilution in PBS/Tw/BSA for 30 min at room temperature. The plates were then incubated with streptavidin-HRP conjugate (Invitrogen) diluted 1:2,000 in TBS/Tw for 15 min, and following with o-phenylenediamine dihydrochloride (OPD) substrate (0.8 mg/ml, Kementec) dissolved in substrate buffer (0.03% freshly prepared H_2O_2 (Sigma-Aldrich) in the dark at room temperature. Color development was stopped by the addition of 100 µl 1 M H_2SO_4, (Sigma-Aldrich) and the plates were read at OD_{492} nm with OD_{600} nm as reference.

Statistical methods

For each continuous outcome variable in the 5- and 10-days studies student's t-test was performed for the comparison between anti-MFAP4 or negative control vehicle-treatment. Mann–Whitney test was performed for comparisons of leach-scoring and Verhofstad scale scoring. For comparisons of effects of anakinra-, vehicle- or anti-MFAP4-treatments in the 28-days study one-way ANOVA with uncorrected Fischer´s least significance difference test (LSD) was used. Results were considered statistically significant if $p < 0.05$. Statistical analyses were performed using GraphPad Prism 10 (https://www.graphpad.com).

Pathway enrichment analyses were based on ranked log2-transformed fold changes (gse function) and unadjusted $p < 0.05$ (unpaired, two-tailed student's t-test for each protein per two-group comparison). The *Benjamini-Hochberg* procedure was applied to correct for multiple testing.

Conference presentation

Part of the work has been presented at the European Pediatric Surgeons' Associations yearly congress in Bologna, June 2024.

Results

Tolerability of local injection of anti-MFAP4 in the anastomosis in early healing phases

In the 5-days study, the mean body weight increase as well as the anastomotic tensile strength as assessed by MATS by day-5 were similar between vehicle and anti-MFAP4 treated groups (Table 1).

The histological Verhofstad scoring was similar between the two groups. No macroscopical findings such as pseudo-diverticulosis, abscesses, leakage, fistulas, or signs of ileus was observed in any of the anastomoses (Table 1).

The addition of aethoxysklerol injections and 5-days longer post-surgery period (10-days study) had no effect on the results (Table 1). The anastomotic index in the 10-days study was similar in the vehicle group and the anti-MFAP4 group with a median of 0.56 in both groups. The scorings of sirius red-determined collagen percentage was similar between the 5-days study, which represents the inflammatory stage where collagen deposition is expected to be limited, and the 10 days-study.

Tolerability of local injection of anti-MFAP4 in the anastomosis in the late healing phase

In the 28-days study we increased the anti-MFAP4 dose to 40 mg/ml to test an escalated dose and we introduced anakinra. We used a variant form of anti-MFAP4, that abolishes potential Fc-mediated undesirable functions, which are immune-activating effects of native antibodies potentially casing cytotoxicity.

Initially, we tested for potential systemic deposition of the locally administered anti-MFAP4 through investigations of samples obtained from lung and artery. We did not observe any detectable anti-MFAP4 (human IgG) in lung and artery, while anti-MFAP4 was detected in the anastomosis 28 days post-surgery (14 days post-injection) (Fig. 2A). Immunostaining of anti-MFAP4 in anastomotic sections from the 28-days study showed no specific staining in vehicle treated sample, and specific staining of elastic fibers (the main location of MFAP4[26,27]) and additional perivascular staining in the anastomotic tissue of anti-MFAP4 treated samples (Fig. 2B-C).

In the 28-days study, the mean body weight increase as well as the anastomotic tensile strength as assessed by MATS were similar between vehicle-, anti-MFAP4- and anakinra-treated groups (Table 2). The anastomotic index was significantly lower both in the anti-MFAP4 treatment group and the anakinra treatment group relative to vehicle control treatment, suggesting that wound contraction was sustained by both treatments (Table 2). Adhesion score was not affected by anti-MFAP4 but was significantly reduced by anakinra. The histological examination showed a significant increase in lymphocytes in both the anakinra- and anti-MFAP4 treatment groups relative to vehicle treatment (Table 2). There were no significant changes in necrosis, polymorphonuclear cells, macrophages, oedema, mucosal epithelium or submucosal muscular layer with either treatment (Table 2). Additionally, there were no macroscopical findings of pseudo-diverticulosis, abscesses, visible leakage, fistulas, or signs of ileus in any of the anastomoses.

Anti-MFAP4 and total collagen deposition in late anastomotic healing phase

The mean anastomotic collagen scoring was approximately doubled in the vehicle-treated 28-days study (Table 2) relative to the earlier healing phase (10-days model, Table 1). Both the positive control anakinra- and anti-MFAP4-treatment resulted in significant reduction of the anastomotic collagen deposition relative to vehicle treatment (Table 2). The anti-MFAP4-treated group showed a significant 23% mean score reduction relative to vehicle treatment. Representative images of collagen deposition in anakinra-, vehicle- and anti-MFAP4-treated groups are shown in Fig. 3.

	Vehicle treatment	Anti-MFAP4 treatment
5-days study	n = 6	n = 7
Baseline body weight	19.1(1.2) kg	20.0(1.9) kg
Body weight increase	2.6(1.2) kg	2.1(0.4) kg
MATS 1	6.3(2.6) N	6.2(2.6) N
MATS 2	10.4(1.6) N	9.4(2.7) N
MATS 3	10.7(1.6)	10.0(3.1) N
Leach score	1.1(1.0)	1.2(0.4)
Necrosis	1.1(0.8)	1.3(0.6)
Polymorphonuclear cells	1.3(0.6)	1.6(0.6)
Lymphocytes	1.3(0.8)	1.3(0.9)
Macrophages	0.2(0.4)	0.1(0.3)
Oedema	0.8(0.8)	1.1(0.8)
Mucosal epithelium	2.3(1.0)	2.4(0.6)
Submucosal muscular layer	1.6(0.7)	1.2(0.6)
Collagen	25.4(8.9)%	23.2(7.5)%
10-days study	+ aethoxysklerol n = 7	+ aethoxysklerol n = 7
Baseline body weight	20.1(1.8) kg	19.0(1.1) kg
Body weight increase	6.9(0.9) kg	7.1(1.1) kg
Anastomotic index	0.56(0.08)	0.56(0.09)
MATS 1	8.9(3.2)	7.5(4.1)
MATS 2	9.1(3.1)	9.5(3.3)
MATS 3	9.6(3.7)	9.7(3.4)
Leach score	1.0(0.6)	0.8(0.4)
Necrosis	1.4(1.0)	1.6(0.5)
Polymorphonuclear cells	1.4(1.0)	1.6(0.7)
Lymphocytes	1.1(0.7)	1.4(0.7)
Macrophages	0.2(0.4)	0.1(0.3)
Oedema	0.8(0.9)	0.7(0.6)
Mucosal epithelium	2.2(1.3)	1.8(1.3)
Submucosal muscular layer	1.7(0.7)	1.6(0.9)
Collagen	24.3(7.0)%	27.3(10.7)%

Table 1. Body weight, anastomotic index, adhesion formation and histochemical scoring in 5- and 10-days studies. Anti-MFAP4 treatment was compared with the negative control vehicle-treatment. Leach scoring and Verhofstad scale scorings were analyzed by Mann–Whitney test. Additional variables were analyzed by t-test. No significant changes were found. Data are mean(SD).

Proteomic changes inferred by anti-MFAP4 treatment in the anastomosis in the late healing phase

A total of 3075 unique proteins were identified by proteomic analysis in all samples (Supplemental Table S1). Nominally regulated proteins from the positive control anakinra- and anti-MFAP4-treated anastomoses are displayed on volcano plots in Fig. 4A-B. Remarkably, the most significantly down-regulated proteins by the positive anti-fibrotic control treatment anakinra included Cartilage Associated Protein (CRTAP), Collagen type II alpha 1 chain (COL2A1) and Collagen type III alpha 1 chain (COL3A1), which are all related with fibrosis (Fig. 4A). This supported the observation of anakinra-mediated reduction of Sirius red-determined fibrosis. Amongst the most significantly up-regulated proteins in the anti-MFAP4 treated groups were markers of epithelial healing; Olfactomedin 4 (OLMF4), which is a marker of intestinal epithelial stem cells[28], and Pytuvate Kinase M (PKM), which may repress apoptosis and facilitate survival of intestinal epithelial cells[29].

We analyzed the proteome data using an unassisted Gene Ontology (GO) enrichment analysis (Supplemental Tables S4 and S5). Several GO terms were nominally regulated in the treatment-groups. The seven most significantly anakinra down-regulated GO terms were related to extracellular matrix- and collagen-formation (Fig. 4C). The GO-term "collagen fibril organization" remained significantly downregulated after controlling for multiple testing. The ten most significantly anakinra up-regulated GO terms included chaperone-related effects, nucleosome related effects and heat-shock protein related effects (response to temperature and heat (Supplemental Table S4)) (Fig. 4D), which are important for proteostasis during mechanical stress[30].

All top-ten anti-MFAP4 up- and down-regulated GO-terms remained significant after correcting for multiple testing. Eight out of the ten most significantly down-regulated GO terms were associated with transcriptional or translational activity (Fig. 4E). The top-ten most significantly up-regulated GO terms were all associated with

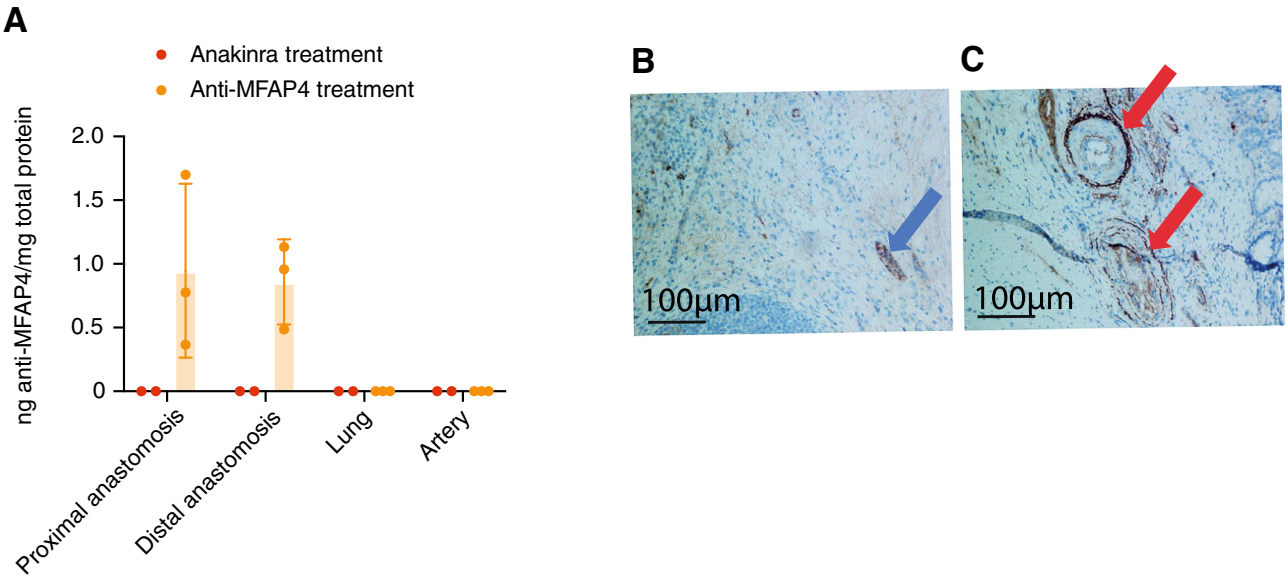

Fig. 2. Anti-MFAP4 detection in intestinal anastomoses, lung tissue and common iliac artery 14 days post-injection of Anakinra or anti-MFAP4 in the anastomotic area. Anti-MFAP4 was locally injected 14-days after surgical formation of intestinal anastomosis in pigs and samples are obtained 28 days post-surgery. (**A**) Anti-MFAP4 was measured by ELISA in protein lysates from two intestinal anastomosis, lung and artery samples treated with either anakinra or anti-MFAP4, (n = 2–3). Data are individual measurement points with mean (SD). (**B**) Unspecific staining of anti-MFAP4 is seen in blood (blue arrow, arterial blood) in vehicle-treated sample. (**C**) anti-MFAP4-treated sample with specific Anti-MFAP4 immunodetection (red arrows). Bar = 100 µm.

	Anakinra treatment	Vehicle treatment	Anti-MFAP4 treatment	*p*-value
28-days study	+ aethoxysklerol N = 9	+ aethoxysklerol N = 9	+ aethoxysklerol N = 9	
Baseline body weight	29.0(3.6) kg	28.2(4.4) kg	29.3(3.2) kg	
Body weight increase	22.4(5.1) kg	24.4(3.9) kg	25.0(4.5) kg	
Anastomotic index	0.62(0.07)[a]	0.72(0.06)	0.63(0.16)[d]	[a]$p = 0.006$, [d]$p = 0.02$
MATS 1	8.3(3.9)	8.5(4.7)	8.8(5.5)	
MATS 2	11.4(3.6)	10.4(3.3)	11.7(4.8)	
MATS 3	13.5(4.1)	12.3(3.7)	13.9(4.7)	
Leach score	0.1(0.3)[b,#]	0.8(1.0)	0.8(1.3)	[b]$p = 0.03$, [#]$p = 0.03$
Necrosis	1.0(0.9)	0.9(0.7)	1.1(1.0)	
Polymorphonuclear cells	0.9(0.6)	0.8(0.7)	1.2(0.9)	
Lymphocytes	0.9(0.6)[d]	0.4(0.6)	1.2(0.7)[e]	[d]$p = 0.04$, [e]$p = 0.0007$
Macrophages	0.4(0.5)	0.3(0.5)	0.7(0.8)	
Oedema	0.9(0.6)	0.8(0.6)	0.6(0.5)	
Mucosal epithelium	0.3(0.8)	0.5(1.0)	0.3(0.5)	
Submucosal muscular layer	1.4(1.0)	1.2(0.7)	1.1(1.0)	
Collagen	36.1(14.2)[c]	52.7(17.8)	40.6(18.0)[f]	[c]$p = 0.004$, [f]$p = 0.03$

Table 2. Body weight, anastomotic index, adhesion formation and histochemical scoring in 28-days study. Effects of anakinra-, vehicle-, or anti-MFAP4-treatments were compared using one-way ANOVA with uncorrected Fischers LSD. Significant *p*-values were observed for [(a-c)]comparisons between anakinra- and vehicle-treatments, [(d-f)]between anti-MFAP4- and vehicle-treatements, or [(#)]comparison between anakinra- and anti-MFAP4-treatements. Data are mean(SD).

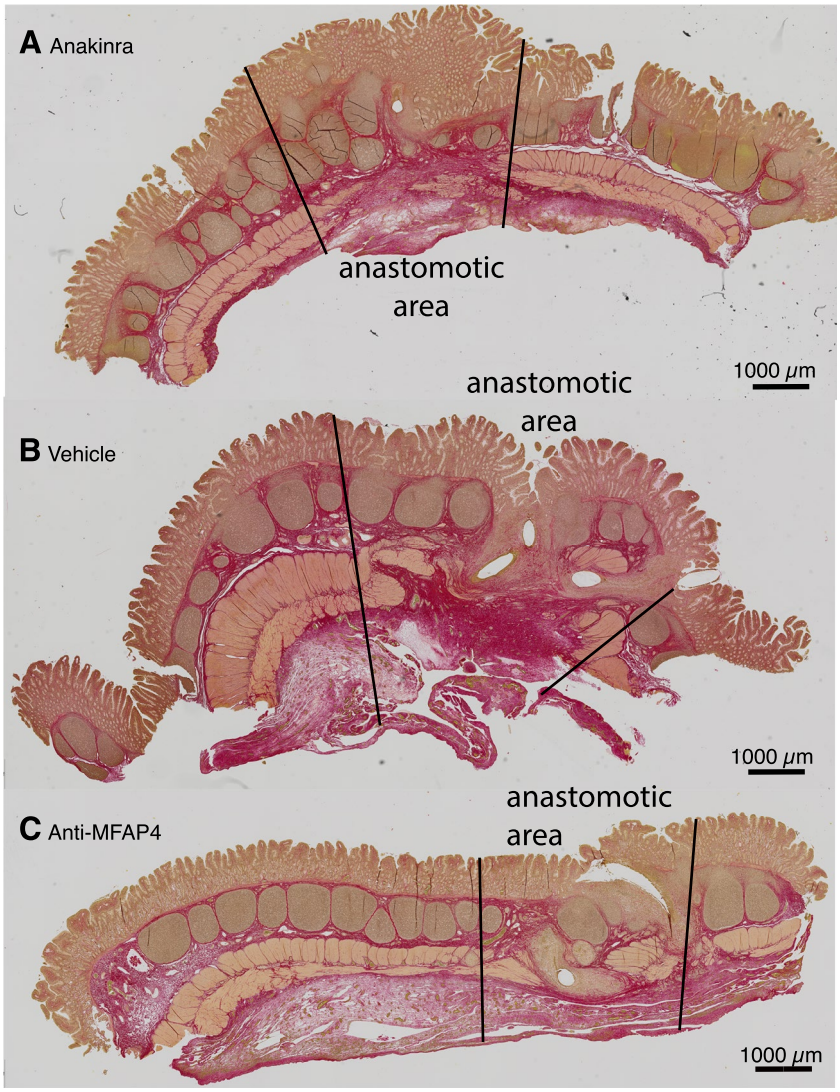

Fig. 3. Collagen deposition in the late anastomotic healing phase. Representative images of collagen deposition (Sirius Red staining) in anastomotic areas in the 28-days study with (**A**) anakinra-treatment, (**B**) vehicle-treatment or (**C**) anti-MFAP4-treatment, respectively. Anakinra, vehicle and anti-MFAP4 were locally injected 14-days post-surgery in the 28-days study. Black lines frame the anastomotic area. Bars = 1000 µm.

muscle contractility or cytoskeletal organization (Fig. 4F). Surprisingly, some GO terms were associated with skeletal muscle, which is not present in the small intestine (I-band, sarcomere, myofibril, Z-disc). However, all the enriched proteins underlying these terms (Supplemental Table S5) are also expressed by smooth muscle cells, albeit with lower transcripts per million relative to skeletal muscle[31]. Therefore, the observed regulations reflect the effects of the contractile apparatus of smooth muscle cells. The data supported that anti-MFAP4-treatment induced SMC-switching from the synthetic phenotype involved in development of fibrostenosis to the contractile phenotype essential for homeostatic gut motor activity.

We analyzed α–SMA immuno-staining in the anastomotic sections and observed a low muscularis propria staining-intensity in the vehicle treated group. The α–SMA immuno-staining was variable between analyzed anastomoses for both the anakinra- and anti-MFAP4-treated groups. Yet, higher intensity of α–SMA immuno-staining was observed in the anakinra-treated group, and the highest α–SMA intensity was observed in the anti-MFAP4-treated group. Representative images are shown in Fig. 5.

Anti-MFAP4 and regulation of lymphocytes

Histochemical evaluation showed that lymphocytes were upregulated by anti-MFAP4 (Table 2) and we therefore looked for proteomic changes related with lymphocytes. Yet, such GO terms related with lymphocytes included downregulation of "gamma-delta T cell activation" (Fig. 4E), and down-regulation of "T-cell proliferation", and "T cell activation" (Supplemental Table S5).

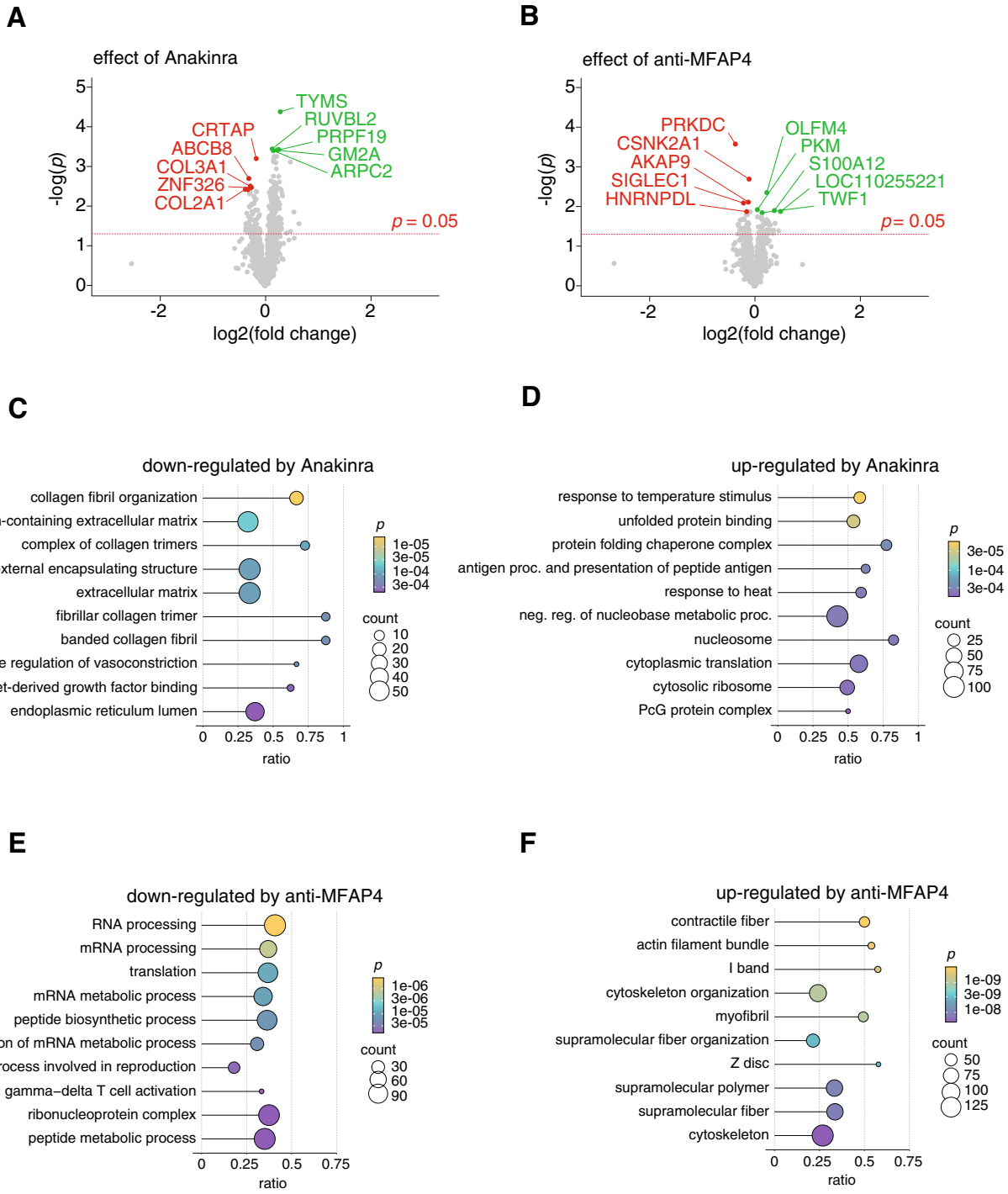

Fig. 4. Proteomic analysis of intestinal anastomosis. Tissue sections from anastomoses obtained from the 28-days study were subjected to proteome analysis. Volcano plots are showing regulation of identified proteins in (**A**) anakinra- (n = 9) or (**B**) anti-MFAP4-treated (n = 9) anastomoses relative to negative control vehicle treated anastomoses (n = 9). The five most significantly down-regulated proteins in volcano plots are shown in red and most significantly up-regulated proteins are shown in green. The ten most significantly up- and down-regulated GO terms are shown for each treatment in (**C**-**D**) anakinra-treated or (**E**–**F**) anti-MFAP4-treated anastomoses. Nominal *p*-values are shown.

Discussion

Observations from the present study support that pharmacological blocking of MFAP4, using anti-MFAP4, has potential as therapeutic intervention to treat fibrostenotic processes in intestinal anastomotic healing. One local dose of 16 mg (20 mg/ml injections) or 32 mg (40 mg/ml injections) anti-MFAP4 did not affect weight gain, the

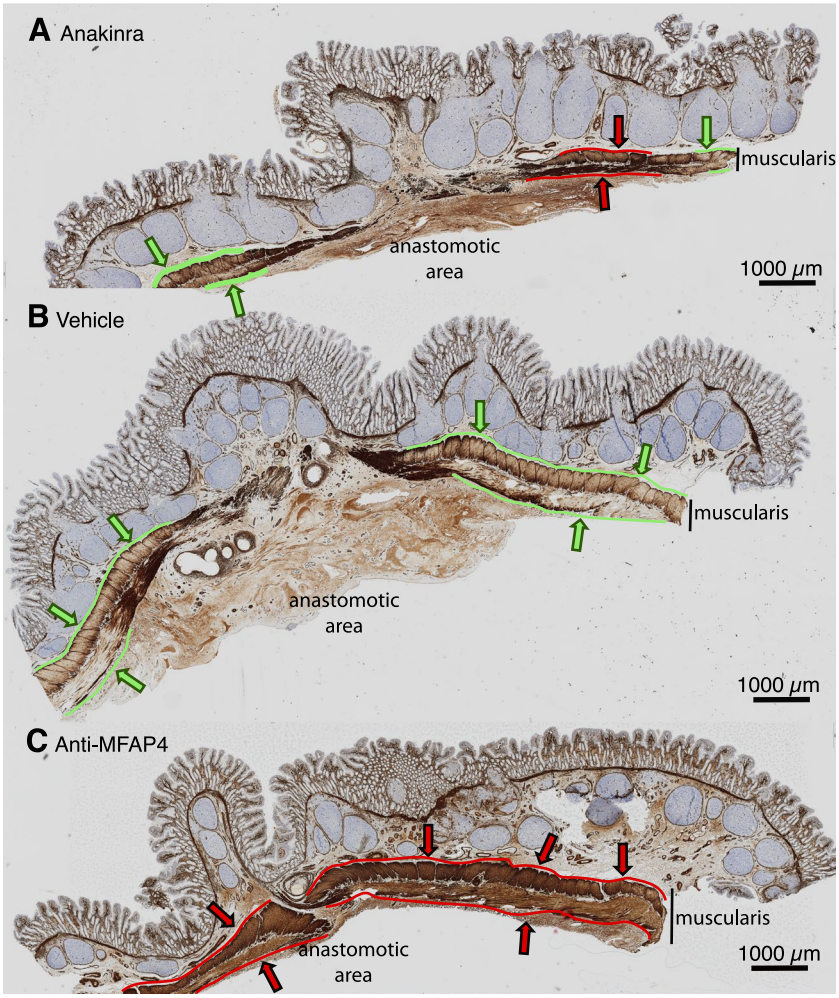

Fig. 5. Anti-MFAP4 induces α–SMA in the muscular layers in the late anastomotic healing phase. Representative images of α–SMA staining (brown staining) of muscular layers (muscularis) in anastomotic and peri-anastomotic areas in 28-days study with (**A**) anakinra treatment, (**B**) vehicle treatment or (**C**) anti-MFAP4 treatment, respectively. Muscularis is broken in the anastomotic area. Green markings indicate areas of intact circular and longitudinal smooth muscle layers of muscularis propria with low α–SMA staining. Red markings indicate areas with high α–SMA staining. Anakinra, vehicle and anti-MFAP4 were locally injected 14-days post-surgery in the 28-days study. Bar = 1000 μm.

anastomotic strength or histochemical evaluation of healing in early and late healing phases, respectively. Local injection with anti-MFAP4 showed reduction of collagen deposition and the anastomotic SMC phenotype was switched from an ECM synthetic phenotype towards a contractile homeostatic phenotype in the late healing phase.

Anti-MFAP4 is raised against human MFAP4. Pigs may be an ideal species for the creation of a large animal model given that their gastrointestinal anatomy closely resembles that of humans[32]. The homology between pig and human MFAP4 is 94% supporting the use of anti-MFAP4 in pigs.

Anti-MFAP4 binds with high affinity to MFAP4, which is embedded in the ECM and therefore it may be retained to a high degree at the injections site. To test if locally injected anti-MFAP4 could reach the circulation and other organs and thereby exert unknown effects tat these sites, we harvested lung and arterial tissue. These tissues represents MFAP4-rich organs. However, we did not observe any anti-MFAP4 deposition in these organs after local injection, whereas approximately 1 ng/ml tissue was retained in the anastomoses 14 days post-injection. In a prior study we observed a duration of efficacy of one dose anti-MFAP4 in reduction of vascular leakage for at least three months[20]. Together, these observations suggest that one dosing of anti-MFAP4 might be retained locally and be sufficient for obtaining a treatment effect through-out a prolonged period. The potential long-term effects of anti-MFAP4, including recurrence of fibrosis beyond 28 days, remain subject for future investigations.

We applied local injection of anti-MFAP4 because other tissues might absorb systemically injected anti-MFAP4. Endoscopic submucosal injection is previously demonstrated as a feasible approach for local delivery of small interfering RNA for other target[33]. Systemic injection might be more directly translatable. However, for systemic injection, it would be required to test systemic tolerability, and a scale-up of our recombinant antibody production would be needed. Consequently, the feasibility of systemic anti-MFAP4 administration remains unknown.

The effective therapeutic dose of anti-MFAP4 for local injection into the pig intestinal anastomosis was unknown when this study was initiated. In a prior study we have observed retinal anti-angiogenic therapeutic efficacy of 2 mg anti-MFAP4 intravitreal injection in non-human primates[20]. This species has a vitreous volume of approximately 2.4 ml[34], and thereby the effective starting dose in that prior study was 0.8 mg/ml. In the present study, we aimed to reach higher doses and locally injected 20 mg/ml (16 mg total) or 40 mg/ml doses (32 mg total) to accommodate for a higher, yet unknown, distribution volume. The 20 mg/ml (16 mg total) dose was chosen to resemble a low dose of 0.5 mg/kg anakinra used in minipigs previously[35] while the 40 mg/ml dose represented a twofold escalation that remained stable when solubilized in the chosen vehicle.

Pro-inflammatory effects of MFAP4 have previously been described[17,26], and consequently anti-MFAP4 might potentially compromise the early inflammatory phase of wound healing. In addition, the anti-angiogenic effects of anti-MFAP4[20] might potentially compromise angiogenesis during the proliferative phase of wound healing. However, we did not see any significant changes in anastomotic tensile strength, or the histological scores following dosing of 20 mg/ml anti-MFAP4 in the early healing phases (5-days and 10-days studies). The tensile strength was measured using MATS test, which is considered appropriate for evaluation of the healing tissue strength[36]. On this basis, we do not expect that anti-MFAP4 compromised early inflammation or angiogenesis to a significant degree.

For testing therapeutic efficacy, we increased the anti-MFAP4 dose to 40 mg/ml in the 28-days study. This higher dose did not weaken the anastomotic strength in the late phase. Any potential effects of 40 mg/ml anti-MFAP4 on in early phase healing were not tested. For the 28-days study, we applied a Fc-neutralized variant of anti-MFAP4 to dampen potential antibody-dependent or complement-dependent cytotoxicity. Moreover, antibodies are expected to arise 9–35 days after antigen exposure in pigs[37]. Therefore, we only applied 14 days of anti-MFAP4-administration to reduce the potential development of anti-antibodies and the associated risk of drug-induced inflammation in the pigs.

While histological scoring supported both anti-MFAP4- and anakinra-induced levels of lymphocytes in the anastomosis, then the proteome analysis supported an immune-suppressive state of the anastomosis in the treated samples. Detailed analysis of lymphocyte populations requires flow- or tissue-cytometry and the immune-modulatory effects of the treatments will be subject for analysis in future studies.

A limitation of the study is the absence of a 14-day baseline control group for the 28-day experiment. However, comparisons between the 10-day and 28-day vehicle-treated groups indicated that the anastomotic index increased over time, while the Leach score and lymphocyte infiltration remained relatively stable. Collagen deposition was higher at day 28 compared with day 10, suggesting progressive fibrosis during this period. Thus, the data support that treatment with anti-MFAP4 and anakinra mitigated collagen accumulation at the anastomotic site.

The normal pig small intestinal anastomosis has non-significantly different collagen volume in the muscularis and subserosa than outside of the anastomosis region when observed in the late healing[38]. We injected aethoxysklerol locally in the anastomotic line at the time of surgery in order to enhance the fibrotic process. The clinical fibrotic effect of aethoxysklerol is not expected to be detectable until week-to-months after sclerotherapy injection. The anti-fibrotic treatment effects were therefore analyzed in the 28-days study.

Dampening of inflammation is expected to reduce fibrogenesis. In line with this, the use of anti-TNF-α antibodies is safe in patients with inflammatory stricturing CD and could decrease the need for surgery over time[39–41]. However, the surgery-free interval is still short and data on anti-fibrotic effect of anti-TNF are lacking[42,43]. In contrast, an anti-fibrotic effect of IL-1-inhibition in the gastrointestinal system and skin is well recognized[44–46] and human IL-1Ra is previously shown to be well tolerated and to show therapeutic efficacy in pigs[47,48]. On this basis we used IL-1RA/anakinra as positive control in the efficacy study.

Anakinra is a recombinantly expressed IL-1 receptor antagonist molecule and was applied as locally injected therapy in the same dose as anti-MFAP4. For clinical use, anakinra is applied by daily subcutaneous injections and such alternative dosing regimen might have provided a higher anti-fibrotic effect than the dosing used in our study. Dysregulation of interleukins decreases the fibrinolytic capacity of the peritoneum, increases adhesion formation, and is initiated in early hemostasis/inflammatory phase[49]. In line with this, anakinra treatment had capacity to reduce adherence formation in our study supported by observations from previous publications applying IL-1R inhibition[44,45]. Our findings demonstrate that anakinra markedly reduces collagen deposition, consistent with its anticipated anti-fibrotic effects. Moreover, anakinra uniquely decreased adhesion formation, highlighting that IL-1 inhibition independently may represent a promising therapeutic approach to improve outcomes following surgical anastomosis.

Semiquantitative collagen scoring, using transmural assessment of Sirius red-determined collagen deposition, is reported to be fast, reliable and reproducible[38] and was applied as a main outcome in our study. However, it considers the entire intestinal wall as a single region of interest and is not as sensitive as stereological assessment of the intestinal anastomotic collagen volume[38]. Nevertheless, semiquantitative collagen scoring showed a significantly reduced anastomotic collagen deposition with both the positive control anakinra-treatment and anti-MFAP4-treatment in the present study. The observed anti-fibrotic activity of anti-MFAP4 is supported by observations of reduced fibrogenesis in gene-deficient mouse models of organ fibrosis[15,17].

Wound contraction refers to the process occurring during initial wound closure and healing, where fibroblasts generate forces that pull the edges of the open wound together to accelerate closure and reduce the resulting scar

size. Scar contraction occurs later, involving the differentiated myofibroblasts that cause shrinkage in a fully healed scar[50]. We assessed wound/scar contraction using x-ray analysis and observed a reduced anastomotic index in the 10-days study. Moreover, both anti-MFAP4- and anakinra-treatment reduced the anastomotic index relative to vehicle control in the 28-days study. Myo(fibroblast)-mediated contraction is dependent upon integrin $\alpha_V b_3$-mediated focal adhesion formation[51,52], but antibody-mediated blocking of MFAP4 is previously shown to reduce focal adhesion formation[26] and could therefore be expected to reduce wound contraction. On the other hand, relaxation of the contraction occurs due to myofibroblast senescence or apoptosis, which is also dependent on integrin $\alpha_V\beta_3$[52]. Our observations suggested that the anti-MFAP4- and anakinra-treatments prolonged the myofibroblast-mediated contraction, while at the same time reducing the collagen-accumulation. Importantly, while myofibroblast contraction is reversible, the deposition and quality of the collagen can make the contraction irreversible[52]. Detailed analysis of the role of anti-MFAP4-treatment in wound/scar contraction would require dynamic, cellular, and ECM constitutional analysis and was not further explored in the present study.

We applied proteome analysis using fixed tissue sections. Formaldehyde fixation limits the extraction efficiency of proteins and thereby the sensitivity. Moreover, proteome analysis is likely to underrepresent ECM proteins, which are often crosslinked and hard to extract even without the fixation. Nevertheless, our analysis showed regulation of collagens in the anakinra treatment group. Each tissue section represented tissue areas being transmural and containing the anastomotic line and additional tissue on each side. The most significantly anti-MFAP4-upregulated proteins were reflecting growth and survival of epithelial cells, and the most significantly anti-MFAP4-regulated GO terms were related to upregulation of the SMC contractile apparatus and down-regulation of transcriptional and translational activity. The main observations from the proteomic analysis supported that anti-MFAP4 induced a phenotypical shift the SMCs from the synthetic/proliferative to the contractile, homeostatic phenotype and α-SMA immuno-staining of the anastomoses supported this observation. This further suggests that the anti-fibrotic effect observed with anti-MFAP4-treatment was secondary to the SMC switch. Integrin $\alpha_V\beta_3$ ligands are previously shown to regulate increased SMC hyperplasia in stricturing Crohn's disease[8]. In parallel, we have previously observed that MFAP4 induced vascular SMC proliferation through integrin $\alpha_V\beta_3$-engagement[26].

Hyperplasia/hypertrophy of the SMC layer contributing to stricture formation is not usually recognized in intestinal anastomoses but often in patients with chronic inflammatory bowel disease per se. It is responsible for intestinal wall thickening and formation of strictures in disease, where chronic inflammation causes a change of metabolism of SMCs that start producing ECM[53]. The observation that anti-MFAP4's major therapeutic effect is related to a beneficial phenotypical switch of SMC may therefore be especially relevant for Crohn's patients. However, the anti-fibrotic effect of anti-MFAP4 may potentially be relevant for various types of patients with increased risk of developing gastrointestinal fibrosis or fibrostenosis.

Overall, the data suggest that both anti-MFAP4 and anakinra reduce collagen deposition at the anastomosis, albeit through distinct mechanisms. Consequently, each agent has potential as an adjunctive therapy to conventional and biologic immunosuppressants, either individually or in combination. Future studies should focus on the adjunctive role of anti-MFAP4 or if it could potentially outperform current anti-inflammatory biologics such as anti-TNF, anti-IL12/23, or anti-integrin agents, which would add additional clinical perspective to the use of anti-MFAP4.

Limitations of the study included that we did not test increasing or repeated dosing of anti-MFAP4, nor dose escalation in early phase healing or systemic injection, and our outcome analysis was based on fixed tissue sections rather than frozen tissue. Moreover, only female pigs were included. Reported sex-specific differences in incidence of IBD, immune responses, and response to therapies[54] may influence the efficacy of anti-fibrotic and anti-inflammatory interventions. Consequently, the observed effects of anti-MFAP4 and anakinra may not fully reflect responses in male animals. Further studies including both sexes are warranted to assess potential differences in treatment response and to enhance the translational relevance of our findings. One general limitation to advancing anti-fibrotic therapies is the lack of a standardized large animal model of fibrosis-driven luminal stricture. Consequently, while our findings demonstrate modulation of fibrotic deposition, they cannot fully predict efficacy in preventing clinically relevant luminal strictures.

Our study was designed to investigate fibrosis deposition in the anastomosis. Others have developed several months long pig-model receiving 5% phenol and 0.2% 2,4,6-trinitrobenzenesulfonic acid solution for repeated submucosal injection to develop true anastomotic fibrostenosis[55] of relevance for potential additional efficacy-testing.

Conclusions

To our knowledge, this is the first study of tolerability and anti-MFAP4-mediated anti-fibrotic effect in post-surgery anastomotic healing. We identified MFAP4 as a new target and pathophysiological factor. Therapeutical blocking of MFAP4 maintained the contractile SMC phenotype and reduced fibrosis. The study further supported previous studies of anakinra-mediated reduction of fibrosis. Our observations warrant further testing of anti-MFAP4 as candidate therapy in Crohn's patients in risk of developing fibrostenosis in post-surgical anastomotic healing.

Data availability

All data underlying this study are available from the corresponding author upon reasonable request.

Received: 15 July 2025; Accepted: 21 November 2025
Published online: 29 November 2025

References

1. Torres, J., Mehandru, S., Colombel, J. F. & Peyrin-Biroulet, L. Crohn's disease. *Lancet* **389**, 1741–1755 (2017).
2. Lin, X. et al. Intestinal strictures in Crohn's disease: a 2021 update. *Therap. Adv. Gastroenterol.* **15**, 17562848221104952 (2022).
3. Khoudari, G. et al. Rates of Intestinal Resection and Colectomy in Inflammatory Bowel Disease Patients After Initiation of Biologics: A Cohort Study. *Clin. Gastroenterol. Hepatol.* **20**, e974–e983 (2022).
4. Poulsen, A. et al. Re-resection Rates and Disease Recurrence in Crohn's Disease: A Population-based Study Using Individual-level Patient Data. *J. Crohns Colitis* **18**, 1631–1643 (2024).
5. Chen, W. et al. Smooth Muscle Hyperplasia/Hypertrophy is the Most Prominent Histological Change in Crohn's Fibrostenosing Bowel Strictures: A Semiquantitative Analysis by Using a Novel Histological Grading Scheme. *J. Crohns Colitis* **11**, 92–104 (2017).
6. Yoo, J. H., Holubar, S. & Rieder, F. Fibrostenotic strictures in Crohn's disease. *Intest. Res.* **18**, 379–401 (2020).
7. Chamley-Campbell, J., Campbell, G. R. & Ross, R. The smooth muscle cell in culture. *Physiol. Rev.* **59**, 1–61 (1979).
8. Flynn, R. S., Murthy, K. S., Grider, J. R., Kellum, J. M. & Kuemmerle, J. F. Endogenous IGF-I and alphaVbeta3 integrin ligands regulate increased smooth muscle hyperplasia in stricturing Crohn's disease. *Gastroenterology* **138**, 285–293 (2010).
9. Blennerhassett, M. G., Vignjevic, P., Vermillion, D. L. & Collins, S. M. Inflammation causes hyperplasia and hypertrophy in smooth muscle of rat small intestine. *Am. J. Physiol.* **262**, G1041-1046 (1992).
10. Thompson, S. K., Chang, E. Y. & Jobe, B. A. Clinical review: Healing in gastrointestinal anastomoses, part I. *Microsurgery* **26**, 131–136 (2006).
11. Morgan, R.B., Shogan, B.D. The science of anastomotic healing. *Semin Colon Rectal Surg.* **33**, (2022).
12. Wulf-Johansson, H. et al. Localization of microfibrillar-associated protein 4 (MFAP4) in human tissues: clinical evaluation of serum MFAP4 and its association with various cardiovascular conditions. *PLoS ONE* **8**, e82243 (2013).
13. Pilecki, B. et al. Characterization of Microfibrillar-associated Protein 4 (MFAP4) as a Tropoelastin- and Fibrillin-binding Protein Involved in Elastic Fiber Formation. *J. Biol. Chem.* **291**, 1103–1114 (2016).
14. Holm, A. T. et al. Characterization of spontaneous air space enlargement in mice lacking microfibrillar-associated protein 4. *Am. J Physiol. Lung. Cell. Mol. Physiol.* **308**, L1114-1124 (2015).
15. Wang, H. B. et al. Deletion of Microfibrillar-Associated Protein 4 Attenuates Left Ventricular Remodeling and Dysfunction in Heart Failure. *J. Am. Heart Assoc.* **9**, e015307 (2020).
16. Wang, H., Liu, M., Wang, X., Shuai, W. & Fu, H. MFAP4 deletion attenuates the progression of angiotensin II-induced atrial fibrosis and atrial fibrillation. *Europace* **24** (2), 340–347 (2022).
17. Pan, Z. et al. MFAP4 deficiency alleviates renal fibrosis through inhibition of NF-κB and TGF-β/Smad signaling pathways. *FASEB J.* **34**(11), 14250–14263 (2020).
18. Nayar, S. et al. A myeloid-stromal niche and gp130 rescue in NOD2-driven Crohn's disease. *Nature* **593**, 275–281 (2021).
19. Estrada, H. Q. et al. Development of a Personalized Intestinal Fibrosis Model Using Human Intestinal Organoids Derived From Induced Pluripotent Stem Cells. *Inflamm Bowel Dis.* **28**, 667–679 (2022).
20. Schlosser, A. et al. Pharmacological blocking of microfibrillar-associated protein 4 reduces retinal neoangiogenesis and vascular leakage. *Molecular Therapy,* **33** (3), 1048–1072 (2025).
21. Kilkenny, C., Browne, W., Cuthill, I. C., Emerson, M. & Altman, D. G. Animal research: reporting in vivo experiments: the ARRIVE guidelines. *Br. J. Pharmacol.* **160**, 1577–1579 (2010).
22. Schlothauer, T. et al. Novel human IgG1 and IgG4 Fc-engineered antibodies with completely abolished immune effector functions. *Protein Eng. Des. Sel.* **29**, 457–466 (2016).
23. Verhofstad, M. H., Lange, W. P., van der Laak, J. A., Verhofstad, A. A. & Hendriks, T. Microscopic analysis of anastomotic healing in the intestine of normal and diabetic rats. *Dis. Colon Rectum.* **44**, 423–431 (2001).
24. Campbell, A. J. et al. A Carrier-Based Quantitative Proteomics Method Applied to Biomarker Discovery in Pericardial Fluid. *Mol. Cell. Proteomics* **23**, 100812 (2024).
25. Wu, T. et al. clusterProfiler 40: A universal enrichment tool for interpreting omics data. *Innovation (Camb)* **2**, 100141 (2021).
26. Schlosser, A. et al. MFAP4 Promotes Vascular Smooth Muscle Migration, Proliferation and Accelerates Neointima Formation. *Arterioscler Thromb. Vasc. Biol.* **36**, 122–133 (2016).
27. Wulf-Johansson, H. et al. Localization of Microfibrillar-Associated Protein 4 (MFAP4) in Human Tissues: Clinical Evaluation of Serum MFAP4 and Its Association with Various Cardiovascular Conditions. *PLoS ONE* **8**, e82243 (2013).
28. van der Flier, L. G., Haegebarth, A., Stange, D. E., van de Wetering, M. & Clevers, H. OLFM4 is a robust marker for stem cells in human intestine and marks a subset of colorectal cancer cells. *Gastroenterology* **137**, 15–17 (2009).
29. Tang, Q. et al. Pyruvate kinase M2 regulates apoptosis of intestinal epithelial cells in Crohn's disease. *Dig. Dis. Sci.* **60**, 393–404 (2015).
30. Hohfeld, J. et al. Maintaining proteostasis under mechanical stress. *EMBO Rep.* **22**, e52507 (2021).
31. Proteinatlas: The Human Protein Atlas. *proteinatlasorg*.
32. Gonzalez, L. M., Moeser, A. J. & Blikslager, A. T. Porcine models of digestive disease: the future of large animal translational research. *Transl. Res.* **166**, 12–27 (2015).
33. Suzuki, K. & Yoneyama, H. New endoscopic approach of anti-fibrotic therapy for inflammatory bowel disease. *Ann. Transl. Med.* **5**, 191 (2017).
34. Glogowski, S., Ward, K. W., Lawrence, M. S., Goody, R. J. & Proksch, J. W. The use of the African green monkey as a preclinical model for ocular pharmacokinetic studies. *J. Ocul. Pharmacol. Ther.* **28**, 290–298 (2012).
35. van Mierlo, G. J. et al. The Gottingen minipig(R) as an alternative non-rodent species for immunogenicity testing: a demonstrator study using the IL-1 receptor antagonist anakinra. *J. Immunotoxicol.* **10**, 96–105 (2013).
36. Bosmans, J. et al. International consensus statement regarding the use of animal models for research on anastomoses in the lower gastrointestinal tract. *Int. J. Colorectal. Dis.* **31**, 1021–1030 (2016).
37. Yoon, K. J. et al. Characterization of the humoral immune response to porcine reproductive and respiratory syndrome (PRRS) virus infection. *J. Vet. Diagn. Invest.* **7**, 305–312 (1995).
38. Kural, T. et al. Histological mapping of healing of the small and large intestine - A quantitative study in a porcine model. *Ann. Anat.* **249**, 152095 (2023).
39. Bouhnik, Y. et al. Efficacy of adalimumab in patients with Crohn's disease and symptomatic small bowel stricture: a multicentre, prospective, observational cohort (CREOLE) study. *Gut* **67**, 53–60 (2018).
40. El-Hussuna, A. et al. No effect of anti-TNF-alpha agents on the surgical stress response in patients with inflammatory bowel disease undergoing bowel resections: a prospective multi-center pilot study. *BMC Surg.* **18**, 91 (2018).
41. Lenti, M. V. & Di Sabatino, A. Intestinal fibrosis. *Mol. Aspects Med.* **65**, 100–109 (2019).
42. Papaconstantinou, I. et al. Effect of infliximab on the healing of intestinal anastomosis. An experimental study in rats. *Int. J. Surg.* **12**, 969–975 (2014).
43. Karakose, O. et al. The Effect of Infliximab on Intestinal Anastomosis Healing in Rats. *Prague Med. Rep.* **117**, 108–116 (2016).
44. Hershlag, A., Otterness, I. G., Bliven, M. L., Diamond, M. P. & Polan, M. L. The effect of interleukin-1 on adhesion formation in the rat. *Am. J. Obstet Gynecol.* **165**, 771–774 (1991).
45. Kaidi, A. A. et al. Preoperative administration of antibodies against tumor necrosis factor-alpha (TNF-alpha) and interleukin-1 (IL-1) and their impact on peritoneal adhesion formation. *Am. Surg.* **61**, 569–572 (1995).
46. Thomay, A. A. et al. Disruption of interleukin-1 signaling improves the quality of wound healing. *Am. J. Pathol.* **174**, 2129–2136 (2009).

47. Chada, M. et al. Anakinra (IL-1R antagonist) lowers pulmonary artery pressure in a neonatal surfactant depleted piglet model. *Pediatr. Pulmonol.* **43**, 851–857 (2008).
48. Morton, A. C. et al. Interleukin-1 receptor antagonist alters the response to vessel wall injury in a porcine coronary artery model. *Cardiovasc. Res.* **68**, 493–501 (2005).
49. Correa-Rovelo, J. M., Villanueva-Lopez, G. C., Medina-Santillan, R., Carrillo-Esper, R. & Diaz-Giron-Gidi, A. Intestinal obstruction secondary to postoperative adhesion formation in abdominal surgery Review. *Cir. Cir.* **83**, 345–351 (2015).
50. Kwan, P., Hori, K., Ding, J. & Tredget, E. E. Scar and contracture: biological principles. *Hand Clin.* **25**, 511–528 (2009).
51. Fiore, V. F. et al. alphavbeta3 Integrin drives fibroblast contraction and strain stiffening of soft provisional matrix during progressive fibrosis. *JCI Insight* **3**, e97597 (2018).
52. Water, L., Varney, S. & Tomasek, J. J. Mechanoregulation of the Myofibroblast in Wound Contraction, Scarring, and Fibrosis: Opportunities for New Therapeutic Intervention. *Adv. Wound Care (New Rochelle)* **2**, 122–141 (2013).
53. Rosendorf, J. et al. Intestinal Anastomotic Healing: What do We Know About Processes Behind Anastomotic Complications. *Front. Surg.* **9**, 904810 (2022).
54. Rustgi, S. D., Kayal, M. & Shah, S. C. Sex-based differences in inflammatory bowel diseases: a review. *Therap. Adv. Gastroenterol.* **13**, 1756284820915043 (2020).
55. Lukas, M. et al. Novel porcine model of Crohn's disease anastomotic stricture suitable for evaluation and training of advanced endoscopic techniques. *Gastrointest Endosc.* **93**, 250–256 (2021).

Acknowledgements

The authors wish to thank veterinarians Charlotte Laurfelt Munch Rasmussen and Louise Langhorn, Diana Bianca Hansen, Pernille Simonsen, Kristoffer Augustesen and laboratory technician Vivi Monrad for their assistance with animal care. Moreover, we wish to thank technicians Lone Christiansen, Department of Pathology at Odense University Hospital and Tine Rasmussen, Institute of Molecular Medicine, University of Southern Denmark, for help and assistance. Generative AI was used to correct syntax of long sentences.

Author contributions

Conceptualization: MBE, NQ and GLS Contributed to study design: MBE, NQ and GLS Methodology and investigations: RRA, JBP, PFHG, CSN, ALK, AFHK, NG, KER, HKH, JK, MD, GIM, LBS and HCB Original draft: RRA and JBP Funding acquisition: MBE and GLS Writing review and editing: All authors. All authors approved the manuscript for publication.

Funding

This work was supported by Novo Nordisk Foundation – Pioneer Innovator grant [NNF22OC0076385]; Clinical center of excellence 'Gastrointestinal Diseases and Malformations in Infancy and Childhood (GAIN) [20/62844], Odense University Hospital; Overlægerådets forskningsfond [A6053], Odense University Hospital; Odense University Hospital Free Funding [A4431]; A.P. Møller Fonden [2024–00886]; A.J. Andersen og Hustrus Fond [01737–0005 FHP].

Declarations

Competing interests

Anders Schlosser and Grith Lykke Sorensen are inventors on U.S. Patent No. 9,988,442 and EP17199552.5 owned by the University of Southern Denmark. Rasmus Refshauge Andresen, Jesper Brandt Pedersen, Paula Frederikke Hellsegg Grünfeld, Charlotte Skoie Nielsen, Anna Lings Kjelgaard, Anders Frederik Højer Kolind, Nils Grimm, Kasper Emil Rosenbech, Henriette Kirkeby Høiberg, Johanne Kalland, Mie Dilling, Gunvor Iben Madsen, Lasse Bach Steffensen, Hans Christian Beck, Sören Möller, Niels Qvist, and Mark Ellebæk have no competing interests.

Additional information

Supplementary Information The online version contains supplementary material available at https://doi.org/10.1038/s41598-025-30123-0.

Correspondence and requests for materials should be addressed to M.E.